Title

Study of B±→J/ψπ± and B±→J/ψK± decays: Measurement of the ratio of branching fractions and search for direct CP-violating charge asymmetries

Journal
Physical Review D, 65(9)

ISSN
2470-0010

Authors
Aubert, B
Boutigny, D
Gaillard, J-M
et al.

Publication Date
2002-05-01

DOI
10.1103/physrevd.65.091101

RAPID COMMUNICATIONS

PHYSICAL REVIEW D, VOLUME 65, 091101(R)

Study of $B^{\pm}\rightarrow J/\psi\pi^{\pm}$ and $B^{\pm}\rightarrow J/\psi K^{\pm}$ decays: Measurement of the ratio of branching fractions and search for direct *CP*-violating charge asymmetries

B. Aubert,[1] D. Boutigny,[1] J.-M. Gaillard,[1] A. Hicheur,[1] Y. Karyotakis,[1] J. P. Lees,[1] P. Robbe,[1] V. Tisserand,[1] A. Palano,[2] A. Pompili,[2] G. P. Chen,[3] J. C. Chen,[3] N. D. Qi,[3] G. Rong,[3] P. Wang,[3] Y. S. Zhu,[3] G. Eigen,[4] B. Stugu,[4] G. S. Abrams,[5] A. W. Borgland,[5] A. B. Breon,[5] D. N. Brown,[5] J. Button-Shafer,[5] R. N. Cahn,[5] A. R. Clark,[5] M. S. Gill,[5] A. V. Gritsan,[5] Y. Groysman,[5] R. G. Jacobsen,[5] R. W. Kadel,[5] J. Kadyk,[5] L. T. Kerth,[5] Yu. G. Kolomensky,[5] J. F. Kral,[5] C. LeClerc,[5] M. E. Levi,[5] G. Lynch,[5] P. J. Oddone,[5] M. Pripstein,[5] N. A. Roe,[5] A. Romosan,[5] M. T. Ronan,[5] V. G. Shelkov,[5] A. V. Telnov,[5] W. A. Wenzel,[5] T. J. Harrison,[6] C. M. Hawkes,[6] D. J. Knowles,[6] S. W. O'Neale,[6] R. C. Penny,[6] A. T. Watson,[6] N. K. Watson,[6] T. Deppermann,[7] K. Goetzen,[7] H. Koch,[7] M. Kunze,[7] B. Lewandowski,[7] K. Peters,[7] H. Schmuecker,[7] M. Steinke,[7] N. R. Barlow,[8] W. Bhimji,[8] N. Chevalier,[8] P. J. Clark,[8] W. N. Cottingham,[8] B. Foster,[8] C. Mackay,[8] F. F. Wilson,[8] K. Abe,[9] C. Hearty,[9] T. S. Mattison,[9] J. A. McKenna,[9] D. Thiessen,[9] S. Jolly,[10] A. K. McKemey,[10] V. E. Blinov,[11] A. D. Bukin,[11] D. A. Bukin,[11] A. R. Buzykaev,[11] V. B. Golubev,[11] V. N. Ivanchenko,[11] A. A. Korol,[11] E. A. Kravchenko,[11] A. P. Onuchin,[11] S. I. Serednyakov,[11] Yu. I. Skovpen,[11] V. I. Telnov,[11] A. N. Yushkov,[11] D. Best,[12] M. Chao,[12] D. Kirkby,[12] A. J. Lankford,[12] M. Mandelkern,[12] S. McMahon,[12] D. P. Stoker,[12] K. Arisaka,[13] C. Buchanan,[13] S. Chun,[13] D. B. MacFarlane,[14] S. Prell,[14] Sh. Rahatlou,[14] G. Raven,[14] V. Sharma,[14] C. Campagnari,[15] B. Dahmes,[15] P. A. Hart,[15] N. Kuznetsova,[15] S. L. Levy,[15] O. Long,[15] A. Lu,[15] J. D. Richman,[15] W. Verkerke,[15] J. Beringer,[16] A. M. Eisner,[16] M. Grothe,[16] C. A. Heusch,[16] W. S. Lockman,[16] T. Pulliam,[16] T. Schalk,[16] R. E. Schmitz,[16] B. A. Schumm,[16] A. Seiden,[16] M. Turri,[16] W. Walkowiak,[16] D. C. Williams,[16] M. G. Wilson,[16] E. Chen,[17] G. P. Dubois-Felsmann,[17] A. Dvoretskii,[17] D. G. Hitlin,[17] S. Metzler,[17] J. Oyang,[17] F. C. Porter,[17] A. Ryd,[17] A. Samuel,[17] M. Weaver,[17] S. Yang,[17] R. Y. Zhu,[17] S. Devmal,[18] T. L. Geld,[18] S. Jayatilleke,[18] G. Mancinelli,[18] B. T. Meadows,[18] M. D. Sokoloff,[18] T. Barillari,[19] P. Bloom,[19] M. O. Dima,[19] W. T. Ford,[19] U. Nauenberg,[19] A. Olivas,[19] P. Rankin,[19] J. Roy,[19] J. G. Smith,[19] W. C. van Hoek,[19] J. Blouw,[20] J. L. Harton,[20] M. Krishnamurthy,[20] A. Soffer,[20] W. H. Toki,[20] R. J. Wilson,[20] J. Zhang,[20] T. Brandt,[21] J. Brose,[21] T. Colberg,[21] M. Dickopp,[21] R. S. Dubitzky,[21] A. Hauke,[21] E. Maly,[21] R. Müller-Pfefferkorn,[21] S. Otto,[21] K. R. Schubert,[21] R. Schwierz,[21] B. Spaan,[21] L. Wilden,[21] D. Bernard,[22] G. R. Bonneaud,[22] F. Brochard,[22] J. Cohen-Tanugi,[22] S. Ferrag,[22] S. T'Jampens,[22] Ch. Thiebaux,[22] G. Vasileiadis,[22] M. Verderi,[22] A. Anjomshoaa,[23] R. Bernet,[23] A. Khan,[23] D. Lavin,[23] F. Muheim,[23] S. Playfer,[23] J. E. Swain,[23] J. Tinslay,[23] M. Falbo,[24] C. Borean,[25] C. Bozzi,[25] S. Dittongo,[25] L. Piemontese,[25] E. Treadwell,[26] F. Anulli,[27,*] R. Baldini-Ferroli,[27] A. Calcaterra,[27] R. de Sangro,[27] D. Falciai,[27] G. Finocchiaro,[27] P. Patteri,[27] I. M. Peruzzi,[27,*] M. Piccolo,[27] Y. Xie,[27] A. Zallo,[27] S. Bagnasco,[28] A. Buzzo,[28] R. Contri,[28] G. Crosetti,[28] M. Lo Vetere,[28] M. Macri,[28] M. R. Monge,[28] S. Passaggio,[28] F. C. Pastore,[28] C. Patrignani,[28] M. G. Pia,[28] E. Robutti,[28] A. Santroni,[28] S. Tosi,[28] M. Morii,[29] R. Bartoldus,[30] R. Hamilton,[30] U. Mallik,[30] J. Cochran,[31] H. B. Crawley,[31] P.-A. Fischer,[31] J. Lamsa,[31] W. T. Meyer,[31] E. I. Rosenberg,[31] G. Grosdidier,[32] C. Hast,[32] A. Höcker,[32] H. M. Lacker,[32] S. Laplace,[32] V. Lepeltier,[32] A. M. Lutz,[32] S. Plaszczynski,[32] M. H. Schune,[32] S. Trincaz-Duvoid,[32] G. Wormser,[32] R. M. Bionta,[33] V. Brigljević,[33] D. J. Lange,[33] M. Mugge,[33] K. van Bibber,[33] D. M. Wright,[33] A. J. Bevan,[34] J. R. Fry,[34] E. Gabathuler,[34] R. Gamet,[34] M. George,[34] M. Kay,[34] D. J. Payne,[34] R. J. Sloane,[34] C. Touramanis,[34] M. L. Aspinwall,[35] D. A. Bowerman,[35] P. D. Dauncey,[35] U. Egede,[35] I. Eschrich,[35] N. J. W. Gunawardane,[35] J. A. Nash,[35] P. Sanders,[35] D. Smith,[35] D. E. Azzopardi,[36] J. J. Back,[36] G. Bellodi,[36] P. Dixon,[36] P. F. Harrison,[36] R. J. L. Potter,[36] H. W. Shorthouse,[36] P. Strother,[36] P. B. Vidal,[36] G. Cowan,[37] S. George,[37] M. G. Green,[37] A. Kurup,[37] C. E. Marker,[37] P. McGrath,[37] T. R. McMahon,[37] S. Ricciardi,[37] F. Salvatore,[37] G. Vaitsas,[37] D. Brown,[38] C. L. Davis,[38] J. Allison,[39] R. J. Barlow,[39] J. T. Boyd,[39] A. C. Forti,[39] J. Fullwood,[39] F. Jackson,[39] G. D. Lafferty,[39] N. Savvas,[39] J. H. Weatherall,[39] J. C. Williams,[39] A. Farbin,[40] A. Jawahery,[40] V. Lillard,[40] J. Olsen,[40] D. A. Roberts,[40] J. R. Schieck,[40] G. Blaylock,[41] C. Dallapiccola,[41] K. T. Flood,[41] S. S. Hertzbach,[41] R. Kofler,[41] V. B. Koptchev,[41] T. B. Moore,[41] H. Staengle,[41] S. Willocq,[41] B. Brau,[42] R. Cowan,[42] G. Sciolla,[42] F. Taylor,[42] R. K. Yamamoto,[42] M. Milek,[43] P. M. Patel,[43] F. Palombo,[44] J. M. Bauer,[45] L. Cremaldi,[45] V. Eschenburg,[45] R. Kroeger,[45] J. Reidy,[45] D. A. Sanders,[45] D. J. Summers,[45] J. Y. Nief,[46] P. Taras,[46] H. Nicholson,[47] C. Cartaro,[48] N. Cavallo,[48,†] G. De Nardo,[48] F. Fabozzi,[48] C. Gatto,[48] L. Lista,[48] P. Paolucci,[48] D. Piccolo,[48] C. Sciacca,[48] J. M. LoSecco,[49] J. R. G. Alsmiller,[50] T. A. Gabriel,[50] J. Brau,[51] R. Frey,[51] E. Grauges,[51] M. Iwasaki,[51] N. B. Sinev,[51] D. Strom,[51] F. Colecchia,[52] F. Dal Corso,[52] A. Dorigo,[52] F. Galeazzi,[52] M. Margoni,[52] G. Michelon,[52] M. Morandin,[52] M. Posocco,[52] M. Rotondo,[52] F. Simonetto,[52] R. Stroili,[52] E. Torassa,[52] C. Voci,[52] M. Benayoun,[53] H. Briand,[53] J. Chauveau,[53] P. David,[53] Ch. de la Vaissière,[53] L. Del Buono,[53] O. Hamon,[53] F. Le Diberder,[53] Ph. Leruste,[53] J. Ocariz,[53] L. Roos,[53] J. Stark,[53] P. F. Manfredi,[54] V. Re,[54] V. Speziali,[54] E. D. Frank,[55] L. Gladney,[55] Q. H. Guo,[55] J. Panetta,[55] C. Angelini,[56] G. Batignani,[56] S. Bettarini,[56] M. Bondioli,[56] F. Bucci,[56] E. Campagna,[56] M. Carpinelli,[56] F. Forti,[56] M. A. Giorgi,[56] A. Lusiani,[56] G. Marchiori,[56] F. Martinez-Vidal,[56] M. Morganti,[56] N. Neri,[56] E. Paoloni,[56] M. Rama,[56] G. Rizzo,[56] F. Sandrelli,[56] G. Simi,[56] G. Triggiani,[56] J. Walsh,[56] M. Haire,[57] D. Judd,[57] K. Paick,[57] L. Turnbull,[57] D. E. Wagoner,[57] J. Albert,[58] P. Elmer,[58] C. Lu,[58] V. Miftakov,[58] S. F. Schaffner,[58] A. J. S. Smith,[58] A. Tumanov,[58] E. W. Varnes,[58] G. Cavoto,[59] D. del Re,[59] R. Faccini,[14,59] F. Ferrarotto,[59] F. Ferroni,[59] E. Lamanna,[59] M. A. Mazzoni,[59] S. Morganti,[59] G. Piredda,[59] F. Safai Tehrani,[59] M. Serra,[59] C. Voena,[59] S. Christ,[60] R. Waldi,[60] T. Adye,[61] N. De Groot,[61] B. Franek,[61] N. I. Geddes,[61] G. P. Gopal,[61] S. M. Xella,[61] R. Aleksan,[62] S. Emery,[62] A. Gaidot,[62] S. F. Ganzhur,[62] P.-F. Giraud,[62] G. Hamel de Monchenault,[62] W. Kozanecki,[62] M. Langer,[62] G. W. London,[62] B. Mayer,[62] B. Serfass,[62] G. Vasseur,[62] Ch. Yèche,[62] M. Zito,[62] M. V. Purohit,[63] H. Singh,[63] A. W. Weidemann,[63] F. X. Yumiceva,[63] I. Adam,[64] D. Aston,[64] N. Berger,[64] A. M. Boyarski,[64] G. Calderini,[64] M. R. Convery,[64] D. P. Coupal,[64] D. Dong,[64] J. Dorfan,[64] W. Dunwoodie,[64] R. C. Field,[64] T. Glanzman,[64] S. J. Gowdy,[64] T. Haas,[64] T. Himel,[64] T. Hryn'ova,[64] M. E. Huffer,[64] W. R. Innes,[64] C. P. Jessop,[64] M. H. Kelsey,[64] P. Kim,[64] M. L. Kocian,[64] U. Langenegger,[64] D. W. G. S. Leith,[64] S. Luitz,[64] V. Luth,[64] H. L. Lynch,[64] H. Marsiske,[64] S. Menke,[64] R. Messner,[64] D. R. Muller,[64] C. P. O'Grady,[64] V. E. Ozcan,[64] A. Perazzo,[64] M. Perl,[64] S. Petrak,[64] H. Quinn,[64] B. N. Ratcliff,[64] S. H. Robertson,[64] A. Roodman,[64] A. A. Salnikov,[64] T. Schietinger,[64] R. H. Schindler,[64] J. Schwiening,[64] A. Snyder,[64] A. Soha,[64] S. M. Spanier,[64] J. Stelzer,[64] D. Su,[64] M. K. Sullivan,[64] H. A. Tanaka,[64] J. Va'vra,[64] S. R. Wagner,[64] A. J. R. Weinstein,[64] W. J. Wisniewski,[64] D. H. Wright,[64] C. C. Young,[64] P. R. Burchat,[65] C. H. Cheng,[65] T. I. Meyer,[65] C. Roat,[65] R. Henderson,[66] W. Bugg,[67] H. Cohn,[67] J. M. Izen,[68] I. Kitayama,[68] X. C. Lou,[68] F. Bianchi,[69] M. Bona,[69] D. Gamba,[69] L. Bosisio,[70] G. Della Ricca,[70] L. Lanceri,[70] P. Poropat,[70] G. Vuagnin,[70] R. S. Panvini,[71] C. M. Brown,[72] P. D. Jackson,[72] R. Kowalewski,[72] J. M. Roney,[72] H. R. Band,[73] E. Charles,[73] S. Dasu,[73] A. M. Eichenbaum,[73] H. Hu,[73] J. R. Johnson,[73] R. Liu,[73] F. Di Lodovico,[73] Y. Pan,[73] R. Prepost,[73] I. J. Scott,[73] S. J. Sekula,[73] J. H. von Wimmersperg-Toeller,[73] S. L. Wu,[73] Z. Yu,[73] T. M. B. Kordich,[74] and H. Neal[74]

(BABAR Collaboration)

[1]*Laboratoire de Physique des Particules, F-74941 Annecy-le-Vieux, France*
[2]*Università di Bari, Dipartimento di Fisica and INFN, I-70126 Bari, Italy*
[3]*Institute of High Energy Physics, Beijing 100039, China*
[4]*University of Bergen, Institute of Physics, N-5007 Bergen, Norway*
[5]*Lawrence Berkeley National Laboratory and University of California, Berkeley, California 94720*
[6]*University of Birmingham, Birmingham, B15 2TT, United Kingdom*
[7]*Ruhr Universität Bochum, Institut für Experimentalphysik 1, D-44780 Bochum, Germany*
[8]*University of Bristol, Bristol BS8 1TL, United Kingdom*
[9]*University of British Columbia, Vancouver, British Columbia, Canada V6T 1Z1*
[10]*Brunel University, Uxbridge, Middlesex UB8 3PH, United Kingdom*
[11]*Budker Institute of Nuclear Physics, Novosibirsk 630090, Russia*
[12]*University of California at Irvine, Irvine, California 92697*
[13]*University of California at Los Angeles, Los Angeles, California 90024*
[14]*University of California at San Diego, La Jolla, California 92093*
[15]*University of California at Santa Barbara, Santa Barbara, California 93106*
[16]*University of California at Santa Cruz, Institute for Particle Physics, Santa Cruz, California 95064*
[17]*California Institute of Technology, Pasadena, California 91125*
[18]*University of Cincinnati, Cincinnati, Ohio 45221*
[19]*University of Colorado, Boulder, Colorado 80309*
[20]*Colorado State University, Fort Collins, Colorado 80523*
[21]*Technische Universitat Dresden, Institut für Kern-und Teilchenphysik, D-01062 Dresden, Germany*
[22]*Ecole Polytechnique, F-91128 Palaiseau, France*
[23]*University of Edinburgh, Edinburgh EH9 3JZ, United Kingdom*
[24]*Elon University, Elon University, North Carolina 27244-2010*
[25]*Università di Ferrara, Dipartimento di Fisica and INFN, I-44100 Ferrara, Italy*
[26]*Florida A&M University, Tallahassee, Florida 32307*
[27]*Laboratori Nazionali di Frascati dell'INFN, I-00044 Frascati, Italy*
[28]*Università di Genova, Dipartimento di Fisica and INFN, I-16146 Genova, Italy*
[29]*Harvard University, Cambridge, Massachusetts 02138*
[30]*University of Iowa, Iowa City, Iowa 52242*
[31]*Iowa State University, Ames, Iowa 50011-3160*
[32]*Laboratoire de l'Accélérateur Linéaire, F-91898 Orsay, France*
[33]*Lawrence Livermore National Laboratory, Livermore, California 94550*
[34]*University of Liverpool, Liverpool L69 3BX, United Kingdom*
[35]*University of London, Imperial College, London, SW7 2BW, United Kingdom*
[36]*Queen Mary, University of London, E1 4NS, United Kingdom*
[37]*University of London, Royal Holloway and Bedford New College, Egham, Surrey TW20 0EX, United Kingdom*
[38]*University of Louisville, Louisville, Kentucky 40292*
[39]*University of Manchester, Manchester M13 9PL, United Kingdom*
[40]*University of Maryland, College Park, Maryland 20742*
[41]*University of Massachusetts, Amherst, Massachusetts 01003*
[42]*Massachusetts Institute of Technology, Laboratory for Nuclear Science, Cambridge, Massachusetts 02139*
[43]*McGill University, Montréal, Quebec, Canada H3A 2T8*

[44]*Università di Milano, Dipartimento di Fisica and INFN, I-20133 Milano, Italy*
[45]*University of Mississippi, University, Mississippi 38677*
[46]*Université de Montréal, Laboratoire René J. A. Lévesque, Montréal, Quebec, Canada H3C 3J7*
[47]*Mount Holyoke College, South Hadley, Massachusetts 01075*
[48]*Università di Napoli Federico II, Dipartimento di Scienze Fisiche and INFN, I-80126, Napoh, Italy*
[49]*University of Notre Dame, Notre Dame, Indiana 46556*
[50]*Oak Ridge National Laboratory, Oak Ridge, Tennessee 37831*
[51]*University of Oregon, Eugene, Oregon 97403*
[52]*Università di Padova, Dipartimento di Fisica and INFN, I-35131 Padova, Italy*
[53]*Universités Paris VI et VII, Laboratoire de Physique Nucléaire H. E., F-75252 Paris, France*
[54]*Università di Pavia, Dipartimento di Elettronica and INFN, I-27100 Pavia, Italy*
[55]*University of Pennsylvania, Philadelphia, Pennsylvania 19104*
[56]*Università di Pisa, Scuola Normale Superiore and INFN, I-56010 Pisa, Italy*
[57]*Prairie View A&M University, Prairie View, Texas 77446*
[58]*Princeton University, Princeton, New Jersey 08544*
[59]*Università di Roma La Sapienza, Dipartimento di Fisica and INFN, I-00185 Roma, Italy*
[60]*Universität Rostock, D-18051 Rostock, Germany*
[61]*Rutherford Appleton Laboratory, Chilton, Didcot, Oxon, OX11 0QX, United Kingdom*
[62]*DAPNIA, Commissarial à l'Energie Atomique/Saclay, F-91191 Gif-sur-Yvette, France*
[63]*University of South Carolina, Columbia, South Carolina 29208*
[64]*Stanford Linear Accelerator Center, Stanford, California 94309*
[65]*Stanford University, Stanford, California 94305-4060*
[66]*TRIUMF, Vancouver, British Columbia, Canada V6T 2A3*
[67]*University of Tennessee, Knoxville, Tennessee 37996*
[68]*University of Texas at Dallas, Richardson, Texas 75083*
[69]*Università di Torino, Dipartimento di Fisica Sperimentale and INFN, I-10125 Torino, Italy*
[70]*Università di Trieste, Dipartimento di Fisica and INFN, I-34127 Trieste, Italy*
[71]*Vanderbilt University, Nashville, Tennessee 37235*
[72]*University of Victoria, Victoria, British Columbia, Canada V8W 3P6*
[73]*University of Wisconsin, Madison, Wisconsin 53706*
[74]*Yale University, New Haven, Connecticut 06511*

(Received 3 August 2001; revised manuscript received 29 January 2002; published 15 April 2002)

We have studied the $B^{\pm}\rightarrow J/\psi\pi^{\pm}$ and $B^{\pm}\rightarrow J/\psi K^{\pm}$ decays using a 20.7 fb^{-1} data set collected with the BABAR detector. We observe a signal of 51 ± 10 $B^{\pm}\rightarrow J/\psi\pi^{\pm}$ events and determine the ratio $\mathcal{B}(B^{\pm}\rightarrow J/\psi\pi^{\pm})/\mathcal{B}(B^{\pm}\rightarrow J/\psi K^{\pm})$ to be $[3.91\pm0.78(\mathrm{stat})\pm0.19(\mathrm{syst})]\%$. The *CP*-violating charge asymmetries for the $B^{\pm}\rightarrow J/\psi\pi^{\pm}$ and $B^{\pm}\rightarrow J/\psi K^{\pm}$ decays are determined to be $\mathcal{A}_{\pi}=0.01\pm0.22(\mathrm{stat})\pm0.01(\mathrm{syst})$ and $\mathcal{A}_{K}=0.003\pm0.030(\mathrm{stat})\pm0.004(\mathrm{syst})$.

DOI: 10.1103/PhysRevD.65.091101

PACS number(s): 13.25.Hw, 12.38.Qk

The decay $B^{\pm}\rightarrow J/\psi\pi^{\pm}$ is both Cabibbo suppressed and color suppressed. If the leading-order tree diagram is the dominant contribution, its branching fraction is expected to be about 5% of the Cabibbo-allowed mode $B^{\pm}\rightarrow J/\psi K^{\pm}$. A comparable prediction can be obtained with a simple model based on the factorization hypothesis [1]. Previous studies of this decay were performed by the CLEO [2] and Collider Detector at Fermilab (CDF) [3] Collaborations. Significant interference terms between the suppressed tree and penguin amplitudes could produce a direct *CP*-violating charge asymmetry in the $B^{\pm}\rightarrow J/\psi\pi^{\pm}$ decays at the few percent level [4]. On the contrary, a negligible direct *CP* violation is expected in the $B^{\pm}\rightarrow J/\psi K^{\pm}$ decays because for $b\rightarrow c\overline{c}\overline{s}$ transitions the standard model predicts that the leading- and higher-order diagrams are characterized by the same weak phase.

In this paper we present a measurement of the ratio of branching fractions $\mathcal{B}(B^{\pm}\rightarrow J/\psi\pi^{\pm})/\mathcal{B}(B^{\pm}\rightarrow J/\psi K^{\pm})$ along with a search for direct *CP* violation in these channels. The data were recorded at the $\Upsilon(4S)$ resonance in 1999–2000 with the BABAR detector at the PEP-II asymmetric-energy $e^{+}e^{-}$ collider at the Stanford Linear Accelerator Center. The integrated luminosity is 20.7 fb^{-1}, corresponding to 22.7 million $B\overline{B}$ pairs. We fully reconstruct $B^{\pm}\rightarrow J/\psi h^{\pm}$ decays, where $h^{\pm}=\pi^{\pm}$, $K^{\pm}$. Signal yields and charge asymmetries are determined from an unbinned maximum likelihood fit that exploits the kinematics of the decay to identify the $\pi^{\pm}$, $K^{\pm}$, and background components in the sample. This kinematic separation is sufficiently good so that no explicit particle identification is required on the charged hadron $h^{\pm}$, thereby simplifying the analysis. At the same time, particle identification can be used to perform a cross-check of the

---

[*] Also at Università di Perugia, Perugia, Italy.

[†] Also at Università della Basilicata, Potenza, Italy.

measurement.

The BABAR detector is described in detail elsewhere [5]. A five-layer silicon vertex tracker (SVT) and a 40-layer drift chamber (DCH), in a 1.5-T solenoidal magnetic field, provide detection of charged particles and measurement of their momenta. The transverse momentum resolution is $\sigma_{p_t}/p_t = (0.13\pm0.01)\%\cdot p_t + (0.45\pm0.03)\%$, where p_t is measured in GeV/c. Electrons are detected in a CsI electromagnetic calorimeter (EMC), while muons are identified in the magnetic flux return system (IFR), which is instrumented with multiple layers of resistive plate chambers. A ring-imaging Cherenkov detector (DIRC) with a quartz bar radiator provides charged particle identification.

An electron candidate is selected according to the ratio of the energy detected in the EMC to track momentum, the cluster shape in the EMC, the energy loss in the DCH, and the DIRC Cherenkov angle, if available. A muon candidate is selected according to the difference between the expected and measured thickness of absorber traversed, the match of the hits in the IFR with the extrapolated track, the average and spread in the number of hits per IFR layer, and the energy detected in the EMC.

$J/\psi\to\mu^+\mu^-$ candidates are constructed from two identified muons with polar angle in the range [0.3, 2.7] radians and with invariant mass $3.06 < M_{\mu^+\mu^-} < 3.14\ \mathrm{GeV}/c^2$. The absolute value of the cosine of the helicity angle of the J/ψ decay is required to be less than 0.9 $J/\psi\to e^+e^-$ candidates are constructed from two identified electrons with polar angle in the range [0.41, 2.409] radians and with invariant mass $2.95 < M_{e^+e^-} < 3.14\ \mathrm{GeV}/c^2$. The absolute value of the cosine of the helicity angle is required to be less than 0.8.

$B^\pm$ candidates are formed from the combination of a reconstructed J/ψ, constrained to the world average mass [6], and a charged track $h^\pm$. A vertex constraint is applied to the reconstructed tracks before computing two kinematic quantities of the $B^\pm$ candidate used to discriminate signal from background. We define the beam energy-substituted mass m_{ES} as

$$m_{\mathrm{ES}} = \sqrt{[(s/2+\mathbf{p_i}\cdot\mathbf{p_B})^2/E_i^2] - |\mathbf{p_B}|^2}, \tag{1}$$

where $\sqrt{s}$ is the total energy of the e^+e^- system in the $\Upsilon(4S)$ rest frame, and $(E_i,\mathbf{p}_i)$ and $(E_B,\mathbf{p_B})$ are the four-momenta of the e^+e^- system and the reconstructed B candidate, both in the laboratory frame. We define the kinematic variable ΔE_π (ΔE_K) as the difference between the reconstructed energy of the $B^\pm$ candidate and the beam energy in the $\Upsilon(4S)$ rest frame assuming $h^\pm = \pi^\pm(K^\pm)$. We require $|\Delta E_\pi| < 120$ MeV, $|\Delta E_K| < 120$ MeV, and $m_{\mathrm{ES}} > 5.2\ \mathrm{GeV}/c^2$. Figure 1 shows the distribution for Monte Carlo simulations of $B^\pm\to J/\psi\pi^\pm$ and $B^\pm\to J/\psi K^\pm$ events in the $(\Delta E_\pi, \Delta E_K)$ plane.

The selected sample contains 1074 $B^\pm\to J/\psi(\to\mu^+\mu^-)h^\pm$ and 1081 $B^\pm\to J/\psi(\to e^+e^-)h^\pm$ candidates. A fit to the ΔE_K distribution with the sum of a Gaussian and a polynomial function, modeling the $B^\pm\to J/\psi K^\pm$ signal and the background contribution is shown in Fig. 2.

The background contaminating the sample is characterized with events in the data that are sufficiently far from the typical signal regions (sidebands of the data sample). We define m_{ES} sideband events by the requirement that $5.2 < m_{\mathrm{ES}} < M_B - 4\sigma(m_{\mathrm{ES}}) = 5.27\ \mathrm{GeV}/c^2$, where M_B is the world average $B^\pm$ mass [6] and $\sigma(m_{\mathrm{ES}})$ is the m_{ES} resolution; their distribution in the $(\Delta E_\pi, \Delta E_K)$ plane is shown in Fig. 3. We define ΔE_K and ΔE_π sideband events by the requirement that $120 > |\Delta E_K| > 4\sigma(\Delta E) = 42$ MeV and $120 > |\Delta E_\pi| > 4\sigma(\Delta E) = 42$ MeV, where $\sigma(\Delta E)$ is the width of the fitted Gaussian in Fig. 2. The distribution in m_{ES} of the sideband events is modeled by an ARGUS function [7], with an additional Gaussian peak in the m_{ES} signal region for events from other $B\to J/\psi X$ decays. The number of background events in this peak has been estimated to be 10 ± 4 with detailed Monte Carlo simulation of inclusive charmonium decays. Figure 4 shows the m_{ES} distribution for the data sample, along with the fit.

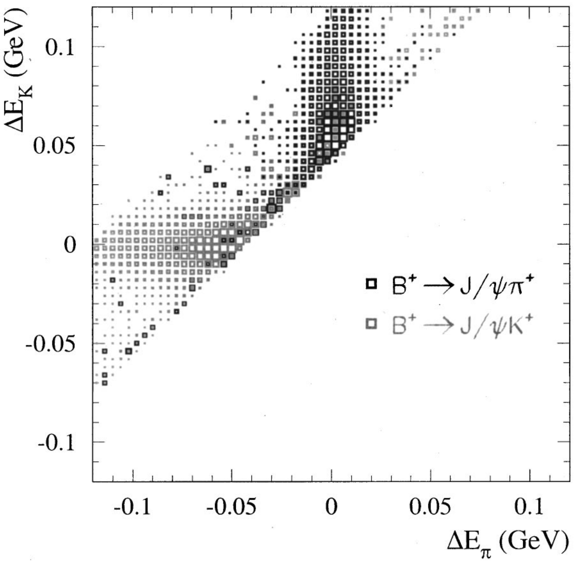

FIG. 1. Distribution of ΔE_K vs ΔE_π for $B^\pm\to J/\psi K^\pm$ and $B^\pm\to J/\psi\pi^\pm$ events from Monte Carlo simulations.

Our fit to the data sample is based on maximizing the following extended likelihood function:

$$L = e^{-\sum_i N_i}\prod_{j=1}^{M}\sum_i P_i(\Delta E_\pi^j, p^j, m_{\mathrm{ES}}{}^j)N_i, \tag{2}$$

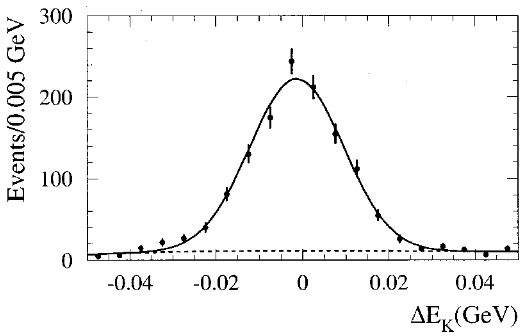

FIG. 2. The ΔE_K distribution and fit for the events in the data sample with $m_{\mathrm{ES}} > 5.27\ \mathrm{GeV}/c^2$. The dashed curve represents the background contribution.

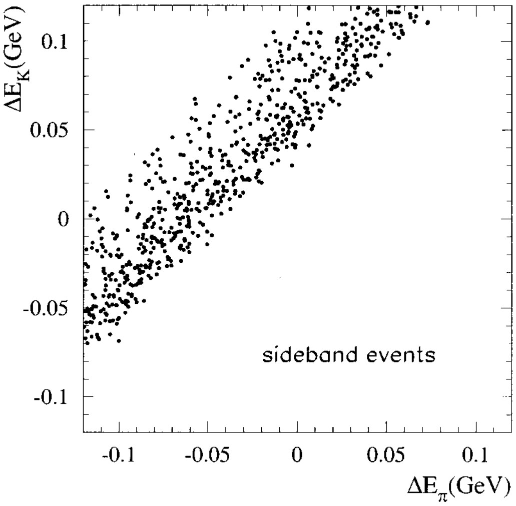

FIG. 3. Distribution of ΔE_K vs ΔE_π for the events in the m_{ES} sideband of the data sample.

where j is the index of the event, i is the index of the hypothesis ($i=\pi,K,bkd$), N_i are the yields for the $B^{\pm}\to J/\psi\pi^{\pm}$, $B^{\pm}\to J/\psi K^{\pm}$, and background events in the sample, and M is the total number of events. The observables ΔE_π, the momentum p of the final-state charged hadron computed in the laboratory frame, and m_{ES} are used as arguments of the probability density functions (PDF) P_i. The PDFs are mainly determined from data with limited input from simulation.

It is useful to define the new variables $D=\Delta E_K-\Delta E_\pi=\gamma(\sqrt{p^2+m_K^2}-\sqrt{p^2+m_\pi^2})$, where γ is the Lorentz boost from the laboratory frame to the $\Upsilon(4S)$ rest frame, and $S=\Delta E_K+\Delta E_\pi=2\Delta E_\pi+D$. These variables have the property that $(\Delta E_\pi,D)$ in the pion hypothesis, $(\Delta E_K,D)$ in the kaon hypothesis and (S,D) in the background hypothesis are uncorrelated at the 1% level. Therefore, with appropriate transformations of variables, each $P_i(\Delta E_\pi,p,m_{\mathrm{ES}})$ can be written as a product of one-dimensional PDFs:

$$P_\pi(\Delta E_\pi,p,m_{\mathrm{ES}})=f_\pi(\Delta E_\pi)g_\pi(D)h_\pi(m_{\mathrm{ES}}),\tag{3}$$

$$P_K(\Delta E_\pi,p,m_{\mathrm{ES}})=f_K(\Delta E_K)g_K(D)h_K(m_{\mathrm{ES}}),\tag{4}$$

$$P_{bkd}(\Delta E_\pi,p,m_{\mathrm{ES}})=f_{bkd}(S)g_{bkd}(D)h_{bkd}(m_{\mathrm{ES}}).\tag{5}$$

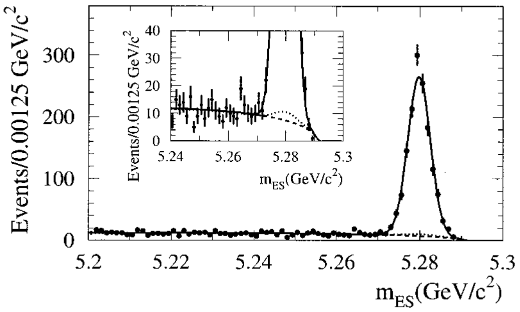

FIG. 4. The m_{ES} distribution and fit for the events in the data sample. The ARGUS (dashed curve) and peaking (dotted curve) components of the background are also displayed.

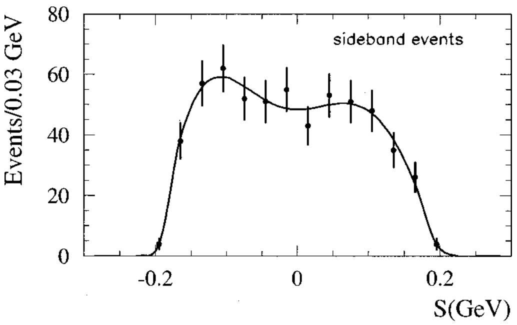

FIG. 5. The S distribution and fit for the events in the m_{ES} sideband of the data sample.

The $f_\pi(\Delta E_\pi)$, $f_K(\Delta E_K)$, $h_\pi(m_{\mathrm{ES}})$, and $h_K(m_{\mathrm{ES}})$ components are the ΔE and m_{ES} resolution functions for the signals. The mean values and the Gaussian widths are allowed to float as free parameters in the likelihood fit and are extracted together with the yields. This strategy reduces the systematic error due to possible inaccuracies of the ΔE and m_{ES} description in Monte Carlo simulations.

The f_{bkd} component is represented by a phenomenological function with eight fixed parameters, all estimated from the distribution of S for the events in the m_{ES} sideband (Fig. 5).

The h_{bkd} component is represented by the sum of an ARGUS and a Gaussian function, with parameters estimated from the distribution of m_{ES} for the events in the ΔE_K and ΔE_π sidebands.

The g components are each represented by a phenomenological function with seven fixed parameters. The parameters are estimated with Monte Carlo simulations for the π and K hypotheses, and with events in the m_{ES} sideband for the background case. A comparison of the D distributions in the three hypotheses shows that this variable, introduced by our procedure for factorizing PDFs, provides little discriminating power.

From the maximum likelihood fit to the selected sample we obtain $N_\pi=52\pm10$, $N_K=1284\pm37$, and $N_{bkd}=819\pm31$. The correlation coefficient between N_π and N_K is -0.04. The confidence level of the fit, defined as the probability to obtain a maximum value of the likelihood smaller than the observed value, is 54%, estimated by Monte Carlo techniques. The statistical significance of the $B^{\pm}\to J/\psi\pi^{\pm}$ signal, evaluated from the change in the maximum value of $\ln L$ when we constrain $N_\pi=0$, is 7.0σ.

The distribution of $\ln(P_\pi/P_K)$ for the sample, after subtraction of the background component in each bin, is shown in Fig. 6. The background distribution is normalized to the number of background events from the fit. The distribution of $\ln(P_\pi/P_K)$ for simulated signal samples, normalized to the yields extracted from the likelihood fit, is also shown. The distribution in ΔE_π for the events in the data sample with $m_{\mathrm{ES}}>5.27$ GeV/c^2 is shown in Fig. 7, along with the likelihood fit result.

Possible biases in the fitting procedure were investigated by performing the fit on simulated samples of known composition and of the same size as the data. The differences, Δ_π and Δ_K, between the extracted and the input values are con-

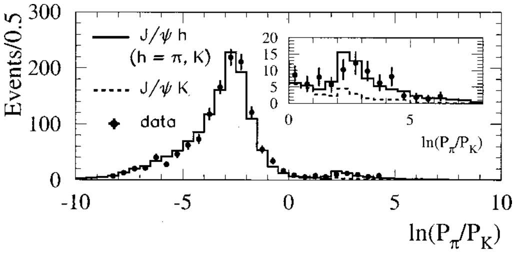

FIG. 6. The $\ln(P_\pi/P_K)$ distribution for events in the data sample (after the subtraction of the background component in each bin) and from Monte Carlo simulations of $B^\pm \to J/\psi\pi^\pm(K^\pm)$ events; the distributions are normalized to the yields extracted from the maximum likelihood fit.

TABLE I. Measurements of $\mathcal{B}(B^\pm \to J/\psi\pi^\pm)/\mathcal{B}(B^\pm \to J/\psi K^\pm)$ obtained with the original (fit 1) and a modified likelihood function (fit 2) that includes particle identification for $h^\pm$. The error on the difference Δ between the two measurements is estimated as $\sigma_\Delta = \sqrt{|\sigma_1^2 - \sigma_2^2|}$.

Sample	Fit 1	Fit 2	Δ/σ_Δ
$J/\psi(\mu^+\mu^-)h^\pm$	$(4.2\pm1.0)\%$	$(4.7\pm1.1)\%$	1.1
$J/\psi(e^+e^-)h^\pm$	$(3.5\pm1.2)\%$	$(4.1\pm1.3)\%$	1.2

sistent with 0. However, we correct the yields for the observed deviations $\Delta_\pi = 1.1 \pm 2.2$ and $\Delta_K = -11.3 \pm 8.8$. The corrected yields are 51 ± 10 and 1296 ± 38 for $J/\psi\pi^\pm$ and $J/\psi K^\pm$, respectively.

The use of particle identification for the charged hadron $h^\pm$ has been investigated by adding to the likelihood, as an additional argument, the Cherenkov angle θ_C measured in the DIRC for this track. The PDFs for the variable θ_C are determined from data and parametrized as Gaussian functions, with mean values and widths that depend on the momentum of the track. A fit with a modified likelihood function is performed with the subsample of events where the particle identification information is available. The ratio of branching fractions is determined separately for the $J/\psi(\mu^+\mu^-)h^\pm$ and $J/\psi(e^+e^-)h^\pm$ samples. A detailed comparison, reported in Table I shows that the addition of particle identification does not significantly change the statistical precision of the results, which are consistent to within 1.6σ.

Based on the fitted event yields, we find the ratio of branching fractions to be

$$\frac{\mathcal{B}(B^\pm \to J/\psi\pi^\pm)}{\mathcal{B}(B^\pm \to J/\psi K^\pm)} = [3.91 \pm 0.78(\text{stat}) \pm 0.19(\text{syst})]\%.$$

The dominant systematic error (0.17%) comes from the uncertainty in the correction factors, Δ_π and Δ_K, due to the limited statistics of the simulated samples. The uncertainty in the fixed parameters of the PDFs, determined by fits to simulated or nonsignal data sets, affects several aspects of the likelihood fit: the characterization of the S and D distributions, the characterization of the m_{ES} distribution for the background (including the fraction of peaking background events), and the fraction of signal events in the tails of the ΔE distribution. This uncertainty contributes 0.07% to the systematic error. Contributions due to any possible difference in the reconstruction efficiencies for $J/\psi\pi^\pm$ and $J/\psi K^\pm$ events are found to be negligible, as are uncertainties due to inaccuracies in the description of the tails of the ΔE resolution function.

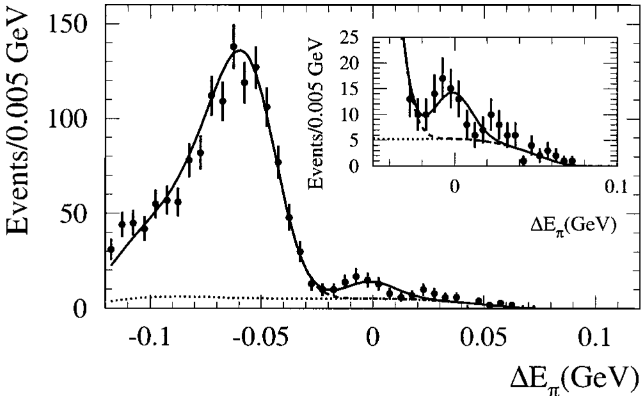

FIG. 7. The ΔE_π distribution for events with $m_{\text{ES}} > 5.27\ \text{GeV}/c^2$ compared with the fit result (solid curve). The dotted curve represents the fitted contribution from the background alone, while the dashed curve represents the fitted contributions from the sum of background and $J/\psi K^\pm$ components. The PDFs of the ΔE_π variable in the $J/\psi K^\pm$ and background hypotheses have been obtained with a numerical integration of the P_i PDFs: $p_K(\Delta E_\pi) = \int f_K(x) g_K(x - \Delta E_\pi) dx$, $p_{bkd}(\Delta E_\pi) = \int f_{bkd}(x + \Delta E_\pi) g_{bkd}(x - \Delta E_\pi) dx$.

Our determination of the ratio of branching fractions is consistent with the expectation reported in [1] and with previous measurements [2,3], but has a substantially lower uncertainty than the world average value of $(5.1 \pm 1.4)\%$ [6].

To study direct *CP* violation in these channels, we modify the likelihood function in Eq. (2) as follows:

$$L' = e^{-\Sigma_i N_i} \prod_{j=1}^{M} \sum_i P_i'(\Delta E_\pi^j, p^j, m_{\text{ES}}^j, q^j) N_i, \qquad (6)$$

where q is the charge of $h^\pm$. We factorize the PDFs as

$$P_i'(\Delta E_\pi, p, m_{\text{ES}}, q) = P_i(\Delta E_\pi, p, m_{\text{ES}}) c_i(q), \qquad (7)$$

where $c_i(q)$ is the probability for the final state charged hadron, in a certain hypothesis, to have charge q. The c_i can be written in terms of the *CP*-violating charge asymmetries $\mathcal{A}_i$, as

$$c_i(q) = \tfrac{1}{2}[(1 - \mathcal{A}_i) f^+(q) + (1 + \mathcal{A}_i) f^-(q)], \qquad (8)$$

where

$$\mathcal{A}_i = \frac{N_i^- - N_i^+}{N_i^- + N_i^+}, \qquad (9)$$

$$f^+(q) = \begin{cases} 1 & \text{if } q = +1, \\ 0 & \text{if } q = -1, \end{cases} \qquad (10)$$

$$f^{-}(q)=\begin{cases}0 & \text{if } q=+1,\\ 1 & \text{if } q=-1.\end{cases} \tag{11}$$

The asymmetry observables $\mathcal{A}_i$ are allowed to float as free parameters in the likelihood fit and are extracted together with the yields.

We impose additional requirements on the charged track $h^{\pm}$ in the events to be used in the fit, selecting only those tracks for which the tracking efficiency has been accurately measured from data. Tracks are required to have a polar angle in the range [0.41, 2.54] radians, to include at least 12 DCH hits, to have $p_t>100\ \mathrm{MeV}/c$, and to point back to the nominal interaction point within 1.5 cm in the vertical plane and within 3 cm along the longitudinal direction. The selected sample contains 982 $B^{-}\to J/\psi h^{-}$ and 970 $B^{+}\to J/\psi h^{+}$ candidates.

From the maximum likelihood fit to the data sample we obtain $\mathcal{A}_{\pi}=0.01\pm0.22$, $\mathcal{A}_{K}=-0.001\pm0.030$, and $\mathcal{A}_{bkd}=0.018\pm0.039$. The correlation coefficient between $\mathcal{A}_{\pi}$ and $\mathcal{A}_{K}$ is -0.03.

The uncertainty in the fixed parameters of the PDFs, determined by fits to simulated or nonsignal data sets, contributes 0.0056 and 0.0002 to the systematic error on $\mathcal{A}_{\pi}$ and $\mathcal{A}_{K}$, respectively. The difference in tracking efficiency between positively and negatively charged tracks—primarily pions—has been studied in hadronic events by comparing the independent SVT and DCH tracking systems. The corrections to the asymmetries $\mathcal{A}_{\pi}$ and $\mathcal{A}_{K}$ are negligible. The uncertainty on the corrections contributes 0.0026 and 0.0020 to the systematic error on $\mathcal{A}_{\pi}$ and $\mathcal{A}_{K}$, respectively. The fake asymmetry due to the different probability of interaction of K^{+} and K^{-} in the detector material before the DCH is estimated to be -0.0039. We correct $\mathcal{A}_{K}$ for this quantity and conservatively assume a contribution of 0.0039 to the systematic uncertainty. This represents the dominant systematic error on $\mathcal{A}_{K}$. A more careful evaluation of the materials and of K^{+}/K^{-} cross-section differences will make it possible to substantially reduce this contribution.

We determine the *CP*-violating charge asymmetries to be

$$\mathcal{A}_{\pi}=0.01\pm0.22(\mathrm{stat})\pm0.01(\mathrm{syst}),$$

$$\mathcal{A}_{K}=0.003\pm0.030(\mathrm{stat})\pm0.004(\mathrm{syst}).$$

These results are consistent with standard model expectations and with the measurement reported in [8].

As a cross-check, $\mathcal{A}_{K}$ has been determined also with a simple analysis based on the counting of $B^{\pm}\to J/\psi K^{\pm}$ signal events in the m_{ES} peak. The result is compatible with the likelihood fit analysis: $A_K=0.005\pm0.030(\mathrm{stat})\pm0.004(\mathrm{syst})$.

We observe no evidence for *CP* violation in $B^{\pm}\to J/\psi\pi^{\pm}$ or $B^{\pm}\to J/\psi K^{\pm}$ decays. These results are statistically limited and can be expected to improve with additional data.

We are grateful for the excellent luminosity and machine conditions provided by our PEP-II colleagues. The collaborating institutions wish to thank SLAC for its support and kind hospitality. This work is supported by DOE and NSF (USA), NSERC (Canada), IHEP (China), CEA and CNRS-IN2P3 (France), BMBF (Germany), INFN (Italy), NFR (Norway), MIST (Russia), and PPARC (United Kingdom). Individuals have received support from the Swiss NSF, A. P. Sloan Foundation, Research Corporation, and Alexander von Humboldt Foundation.

---

[1] M. Neubert and B. Stech, in *Heavy Flavours II*, edited by A. J. Buras and M. Lindner (World Scientific, Singapore, 1988), p. 345.
[2] CLEO Collaboration, M. Bishai *et al.*, Phys. Lett. B **369**, 189 (1996).
[3] CDF Collaboration, F. Abe *et al.*, Phys. Rev. Lett. **77**, 5176 (1996).
[4] I. Dunietz, Phys. Lett. B **316**, 561 (1993).
[5] BABAR Collaboration, B. Aubert *et al.*, Nucl. Instrum. Methods Phys. Res. A **479**, 1 (2002).
[6] Particle Data Group, D. E. Groom *et al.*, Eur. Phys. J. C **15**, 1 (2000).
[7] ARGUS Collaboration, H. Albrecht *et al.*, Phys. Lett. B **185**, 218 (1987).
[8] CLEO Collaboration, G. Bonvicini *et al.*, Phys. Rev. Lett. **84**, 5940 (2000).